

# A Global Potential Analysis of the $^{16}\text{O}+^{28}\text{Si}$ Reaction Using a New Type of Coupling Potential

I. Boztosun <sup>†</sup>

*Department of Physics, Erciyes University, 38039 Kayseri Turkey*

W.D.M. Rae

*Department of Nuclear Physics, University of Oxford, Keble Road, Oxford OX1 3RH UK*

(November 10, 2018)

## Abstract

A new approach has been used to explain the experimental data for the  $^{16}\text{O}+^{28}\text{Si}$  system over a wide energy range in the laboratory system from 29.0 to 142.5 MeV. A number of serious problems has continued to plague the study of this system for a couple of decades. The explanation of anomalous large angle scattering data; the reproduction of the oscillatory structure near the Coulomb barrier; the out-of-phase problem between theoretical predictions and experimental data; the consistent description of angular distributions together with excitation functions data are just some of these problems. These are long standing problems that have persisted over the years and do represent a challenge calling for a consistent framework to resolve these difficulties within a unified approach. Traditional frameworks have failed to describe these phenomena within a single model and have so far only offered different approaches where these difficulties are investigated separately from one another. The present work offers a plausible framework where all these difficulties are investigated and answered. Not only it improves the simultaneous fits to the data of these diverse observables, achieving this within a unified approach over a wide energy range, but it departs for its coupling potential from the standard formulation. This new feature is shown to improve consistently the agreement with the experimental data and has made major improvement on all the previous coupled-channels calculations for this system.

## Keywords:

$^{16}\text{O}+^{28}\text{Si}$  Reaction, coupled-channels model/methods/calculations, optical model, elastic and inelastic scattering, anomalous large angle scattering (ALAS), excitation function.

---

<sup>†</sup>Present address: Computational Mathematics Group, School of Computer Science and Mathematics, University of Portsmouth, Portsmouth PO1 2EG UK

## I. INTRODUCTION

Since the first observation of the unexpectedly large cross-section near  $\theta_{CM}=180^\circ$  for the elastic and the inelastic scattering between light and medium heavy nuclei [1], considerable experimental and theoretical efforts have been devoted to the systematic studies of this phenomenon and related aspects.

The physical origin of the observed structure is not yet fully understood [2,3] and presents a challenge to different approaches that have been proposed to explain it. These approaches range from the occurrence of possibly overlapping shape resonances [4] and the scattering from surface-transparent optical potentials [5] to more exotic effects like explicit parity dependence of the ion-ion potential [6,7]. At present, none of these approaches provides a consistent explanation for all the existing data for this system.

Consequently, the following problems continue to exist for this reaction [8–11]: (1) the explanation of anomalous large angle scattering data; (2) the reproduction of the oscillatory structure near the Coulomb barrier; (3) the out-of-phase problem between theoretical predictions and experimental data; (4) the consistent description of angular distributions together with excitation functions data; (5) the deformation parameters ( $\beta$  values): previous calculations require  $\beta$  values that are at variance with the empirical values and are physically unjustifiable.

The elastic and inelastic scattering data of the  $^{16}\text{O}+^{28}\text{Si}$  system have been studied extensively and some of the above-mentioned problems could not be accounted for [12–17]. The most extensive study for this system was carried out by Kobos and Satchler [12] who used a double folding potential with two small additional *ad-hoc* potentials to reproduce the measured elastic scattering data. Without two small additional potentials, they observed that the theoretical calculations and the experimental data were completely out-of-phase and could not reproduce the experimental data.

Therefore, building on two previous papers [8,9], which were outstandingly successful in explaining the experimental data for the  $^{12}\text{C}+^{12}\text{C}$  and  $^{12}\text{C}+^{24}\text{Mg}$  reactions which both have been intensively investigated over the years [14–19], we investigate the elastic and inelastic scattering of  $^{16}\text{O}+^{28}\text{Si}$  system from 29.0 MeV to 142.5 MeV. The excitation functions for the ground and the first excited states have also been analyzed over this energy range. In this paper, our aim is to reproduce all the experimental data with empirical  $\beta$  value.

In the next section, we first introduce the standard coupled-channels model and then show the results of these analyzes in section III from  $E_{Lab}=29.0$  MeV to 142.5 MeV. In section IV, we introduce a new coupling potential to analyze the experimental data in the same energy range and show the results of these new coupled-channels calculations. Finally, section V is devoted to our summary and conclusion.

## II. THE STANDARD COUPLED-CHANNELS CALCULATIONS

In the present coupled-channels calculations, we describe the interaction between  $^{16}\text{O}$  and  $^{28}\text{Si}$  nuclei with a deformed optical potential. The real potential is assumed to have the square of a Woods-Saxon shape:

$$V_N(r) = \frac{-V_0}{(1 + \exp(r - R)/a)^2} \quad (1)$$

with  $V_0=706.5$  MeV,  $R=r_0(A_P^{1/3}+A_T^{1/3})$  with  $r_0=0.7490$  fm and  $a=1.40$  fm. The parameters of the real potential are fixed as a function of energy and are not changed in the present calculations although it was observed that small changes could improve the quality of the fits. The Coulomb potential with a radius of 5.56 fm is also added.

The imaginary part of the potential is taken as the sum of a Woods-Saxon volume and surface potentials:

$$W(r) = -W_V f(r, R_V, a_V) + 4W_S a_S df(r, R_S, a_S)/dr \quad (2)$$

$$f(r, R, a) = \frac{1}{1 + \exp((r - R)/a)} \quad (3)$$

with  $W_V=59.9$  MeV,  $a_V=0.127$  fm and  $W_S=25.0$  MeV,  $a_S=0.257$  fm. These parameters are also fixed in the calculations and only their radii increase linearly with energy according to the following formulae:

$$R_V = 0.061E_{CM} - 0.44 \quad (4)$$

$$R_S = 0.241E_{CM} - 2.19 \quad (5)$$

The real and imaginary potentials are shown in figure 1 for  $E_{Lab}= 41.17$  MeV. The sum of the nuclear, Coulomb and the centrifugal potentials is also shown in the same figure for the orbital angular momentum quantum number,  $l = 10$ . The superposition of the attractive and repulsive potentials results in the formation of a potential pocket, which the width and depth of the pocket depend on the orbital angular momentum. This pocket is very important for the interference of the barrier and internal waves, which produces the pronounced structure in the cross-section. The effect of this pocket can be understood in terms of the interference between the internal and barrier waves that correspond to a decomposition of the scattering amplitude into two components, the inner and external waves [20,21].

The relative significance of the volume and surface components of the imaginary potential has also been examined for all the energies considered. For higher energies, omitting the volume term predominantly affects the amplitude of the cross-section at large angles. However, this effect is small and negligible at lower energies. Omitting the surface term increases the cross-sections at large angles which are as much as two orders of magnitude. It is observed that this term has a significant effect at all the energies considered.

Since the target nucleus  $^{28}\text{Si}$  is strongly deformed, it is essential to treat its collective excitation explicitly in the framework of the coupled-channels formalism. It has been assumed that the target nucleus has a static quadrupole deformation, and that its rotation can be described in the framework of the collective rotational model. It is therefore taken into account by deforming the real optical potential in the following way

$$R(\theta, \phi) = r_0 A_P^{1/3} + r_0 A_T^{1/3} [1 + \beta_2 Y_{20}(\theta, \phi)] \quad (6)$$

where  $P$  and  $T$  denote the projectile and target nuclei respectively and  $\beta_2=-0.64$  is the deformation parameter of  $^{28}\text{Si}$ . This value is actually larger than the value calculated from

the known B(E2). However this larger  $\beta_2$  was needed to fit the magnitude for the  $2^+$  state data as discussed in the next sections.

In the present calculations, the first two excited states of the target nucleus  $^{28}\text{Si}$ , *i.e.*  $2^+$  (1.78 MeV) and  $4^+$  (4.62 MeV), are included and the  $0^+-2^+-4^+$  coupling scheme is employed. The reorientation effects for  $2^+$  and  $4^+$  excited states are also included. The inclusion of the  $2^+$  and  $4^+$  excited states has important effects as their effects change the elastic scattering fits substantially. These effects confirm that it is essential to use the coupled-channels method in the case where one of the nuclei in the reaction is strongly deformed. Extensively modified version of the code *CHUCK* [22] has been used for the all calculations.

### III. RESULTS

Using this standard coupled-channels model, the results for the ground and first excited states are shown in figures 2, 3, 4 and 5. It should be stressed that very close fits to the experimental data at forward, backward and intermediate angles were obtained without applying any *ad-hoc* procedures other than increasing the  $\beta_2$  value (see  $\chi^2$  values in table I). In general, the previous coupled-channels calculations aiming to explain the structures at large angles obtained rather poor fits at forward angles or vice versa. Even when the forward and backward angles were fitted, the intermediate angles were not [1,23].

However, there are problems in our first excited state results. The magnitude of the cross-sections and the phase of the oscillations are obtained correctly at most angles. However, when one looks at the  $2^+$  state results in detail, it is apparent that the experimental data and our predictions are out-of-phase towards large angles at higher energies. This problem was also found in earlier coupled-channels calculations for this system [1,13,23].

When studying this reaction systematically in a wide energy range, we came across several problems: The first problem relates to the oscillatory structure and to the backward rise in the cross-section at large angles for which the standard coupled-channels model provides a solution.

The second problem pertains to the calculation of the first excited state cross-section. Using the exact  $\beta$  value, we observed that the calculations underestimated the experimental data, a phenomenon confirmed by other works which assert that in the coupled-channels or DWBA calculations, one has to increase or decrease the deformation parameter( $\beta$ ) to be able to get agreement with the measured experimental data and that the choice of the  $\beta$  value is somehow arbitrary in fitting the data. Therefore, we also adopted to increase the  $\beta$  value.

The third problem arises due to Blair's phase rule [24] which states that 'the oscillations for even- $l$  transfer are out-of-phase with those for elastic scattering, while those for odd- $l$  transfer are in phase'. These experimental data obey this rule at numerous energies, except the energies around  $E_{Lab}\sim 35.0$  MeV (see figures 3 and 5). While the measured cross-section for the ground state has maxima at  $\sim 180^\circ$ , it has also maxima at  $\sim 180^\circ$  for the  $2^+$  state whereas, it should have minima  $\sim 180^\circ$  according to the Blair's phase rule.

The theoretical predictions are completely out-of-phase around these energies for the  $2^+$  state although they fit the ground state data. This problem is also clearly observed in the  $180^\circ$  excitation function of the  $2^+$  state as shown in figure 6. The magnitudes of our calculations are also at least twice bigger than the experimental data at lower energies.

Our coupled-channels calculations showed that the threshold energy is  $E_{Lab} \sim 35.0$  MeV. It was also reported [25] that the irregular behavior of the experimental data starts beyond this energy. No coupled-channels calculation has been carried out below and above this energy simultaneously. However, research has been conducted and studies have been published pertaining to below or above this energy ( $E_{Lab} \sim 35.0$  MeV).

In the past, a number of models have been proposed in order to solve the above-mentioned problems, ranging from isolated resonances [4,26] to cluster exchange between the projectile and target nucleus [15,27] (see [2] for a detailed discussion). We have attempted to overcome these problems by modifying the shape and the parameters of the real potential as well as the parameters and the shape of the imaginary potential. These modifications in the real and imaginary potentials improved the  $180^\circ$  excitation function. However, we were unable to fit individual angular distributions and excitation functions simultaneously over the whole energy range.

We then sought to include the  $6^+$  excited state. The inclusion of one additional excited state weakened the imaginary potential and this was useful to infer what the shape of the imaginary potential should be. Nevertheless, we were unable to include it in the final stage since it created a numerical accuracy/instability problem in the code. We finally changed the  $\beta_2$  value and included a  $\beta_4$  deformation. However, varying the value of the  $\beta_2$  and the inclusion of the  $\beta_4$  did not solve the problems.

In summary, these attempts failed to provide a wholistic solution to the above-mentioned problems. We were unable to explain the elastic and inelastic scattering data as well as their  $180^\circ$  excitation functions simultaneously.

#### IV. NEW COUPLING POTENTIAL

The limitations of the standard coupled-channels theory in the analysis of this reaction has been well established by both our analyzes and the works published so far. We came across the same type of failure of the standard coupled-channels method in explaining the experimental data for the  $^{12}\text{C}+^{12}\text{C}$  and  $^{12}\text{C}+^{24}\text{Mg}$  reactions.

In order to explain the experimental data for these systems, we had to introduce a new type of coupling potential, which is a second-derivative coupling potential used in the place of the usual first derivative coupling potential. This new coupling potential has successfully explained the scattering observables of these two reactions over wide energy ranges and has made major improvement on the all the previous coupled-channels calculations for these systems. The reason and a possible interpretation of such a new coupling potential have been discussed in the two previous papers [8,9].

Building on these two previous papers, here we use a new second-derivative coupling potential to find a global solution to the problems that  $^{16}\text{O}+^{28}\text{Si}$  reaction manifests. This new coupling potential is displayed in comparison with the standard coupling potential in figure 7. It is parameterized accurately as the second-derivative of the Woods-Saxon shape in the following form:

$$V_C(r) = \frac{-V_{C_0} e^x (e^x - 1)}{a^2 [1 + e^x]^3} \quad (7)$$

where  $x = (r - R)/a$  and  $V_{C_0} = 155.0$  MeV,  $R = 4.16$  fm and  $a = 0.81$  fm.

In the new coupled-channels calculations, the real and imaginary potentials have the same shapes as given by the equations 1 and 2 and the same potential parameters are used except for the depth of the real potential and the  $\beta_2$  value. They have to be readjusted as  $V_0=750.5$  MeV and  $\beta_2=-0.34$ , which corresponds to the exact value derived from the life time of the  $2^+$  state [23,28,29].

We have analyzed the experimental in the same energy range using this empirical  $\beta_2$  value and the results of the new coupled-channels calculations are shown in figures 8, 9 and 10 for the ground state. Figure 11 presents the inelastic scattering while figure 12 shows the  $180^\circ$  excitation function for the ground and first excited states.

This new coupling potential solves the out-of-phase problem as shown in figure 12 and fits the ground state data and the  $180^\circ$  excitation functions simultaneously. A comparison is given for the  $2^+$  excited state in figure 12. While the standard coupling potential is out-of-phase with the measured one, this new coupling potential significantly improves the agreement with the experimental data and solves the out-of-phase problem.

It is striking that the phase variation and the absolute magnitude of the inelastic cross-sections for all energies are correctly accounted for with this model. In contrast to the predictions of the standard coupled-channels calculations, the magnitude of the  $2^+$  excited state data at lower and intermediate energies where we have available experimental data for the individual angular distributions are fitted well. The comparison of the  $\chi^2$  values with the standard one is given in table I.

Finally, table II shows the volume integrals of the real and surface and volume imaginary potentials. The volume integrals of the real and imaginary potentials are calculated by using following formulae:

$$\begin{aligned} J_V(E) &= \left[ \frac{4\pi}{A_P A_T} \int_0^R V(r, E) r^2 dr \right] \\ J_W(E) &= \left[ \frac{4\pi}{A_P A_T} \int_0^R W(r, E) r^2 dr \right] \end{aligned} \quad (8)$$

The radii of the imaginary potentials are calculated from equations 4 and 5. It is seen from table II that the potentials fulfill the dispersion relations and the agreement between  $r_{W_{S,V}}$  and  $J_{W_{S,V}}$  is very good.

## V. SUMMARY

We have shown a consistent description of the elastic and inelastic scattering of the  $^{16}\text{O}+^{28}\text{Si}$  system from 29.0 MeV to 142.5 MeV in the laboratory system by using the standard and new coupled-channels calculations. In the introduction, we presented the problems that this reaction manifests. We attempted to find a consistent solution to these problems. However, within the standard coupled-channels method, we failed, as others did, to describe certain aspects of the data, in particular, the magnitude of the  $2^+$  excitation inelastic scattering data although the optical model and coupled-channels models explain perfectly some aspects of the elastic scattering data. In order to reproduce the first excited state ( $2^+$ ) data in the standard coupled-channels calculations, we were compelled to increase the value of nuclear deformation and such arbitrary uses of  $\beta$  have been practiced in the past without

giving any physical justifications other than stating it is required to fit the experimental data. Although we obtained a reasonable agreement between the experimental data and theoretical calculations for the ground and  $2^+$  state data, the standard coupled-channels method have totally failed in providing simultaneous fits to the individual angular distributions and  $180^\circ$  excitation functions and could not solve the out-of-phase problem between the theory and experimental data for these states.

We have, however, obtained excellent agreement with the experimental data over the whole energy range studied by using a new coupling potential, which has been outstandingly successful in explaining the experimental data for the the  $^{12}\text{C}+^{12}\text{C}$  [8] and  $^{12}\text{C}+^{24}\text{Mg}$  [9] systems over wide energy ranges. The comparison of the results indicates that a global solution to the problems relating to the scattering observables of this reaction over a wide energy range has been provided by this new coupling potential. However, it is not possible at present to provide a solid theoretical foundation and further work in order to derive this term from a microscopic viewpoint is still under-progress. Any insights that would lead to progress in this direction will be greatly welcome in the future.

## VI. ACKNOWLEDGMENTS

Authors wish to thank Doctors Y. Nedjadi, S. Ait-Tahar, B. Buck, A. M. Merchant, Professor B. R. Fulton and Ayşe Odman for valuable discussions and encouragements. I. Boztosun also would like to thank the Turkish Council of Higher Education (YÖK) and Erciyes University, Turkey, for their financial support.

## REFERENCES

- [1] P. Braun-Munzinger, G.M. Berkowitz, T.M. Cormier, C.M. Jachcinski, J.W. Harris, J. Barrette and M.J. Levine, *Phys. Rev. Lett.* **38** (1977) 944.
- [2] P. Braun-Munzinger and J. Barrette, *Phys. Reports* **87** (1982) 209.
- [3] I. Boztosun and W.D.M. Rae, *Proceedings of the 7<sup>th</sup> International Conference on Clustering Aspects of Nuclear Structure and Dynamics*, Edited by M. Korolija, Z. Basrak and R. Caplar, World-Scientific-2000 (143).
- [4] J. Barrette, M.J. LeVine, P. Braun-Munzinger, G.M. Berkowitz, M. Gai, J.M. Harris and C.W. Jachcinski, *Phys. Rev. Lett.* **40** (1978) 445.
- [5] S. Kahana, B.T. Kim and M. Mermaz, *Phys. Rev. C* **20** (1979) 2124.
- [6] D. Dehnhard, V. Shkolnik and M.A. Franey, *Phys. Rev. Lett.* **40** (1978) 1549.
- [7] S. Kubono, P.D. Bond and C.E. Thorn, *Phys. Lett.* **81B** (1979) 140.
- [8] I. Boztosun and W.D.M. Rae, *Phys. Rev. C* **63** (2001) 054607.
- [9] I. Boztosun and W.D.M. Rae, *Phys. Rev. C* **64** (2001) 054607.
- [10] I. Boztosun, DPhil Thesis, Oxford University, 2000;  
I. Boztosun, accepted for the publication in *Phys. of Atomic Nuclei (Yadernaya Fizika)*.
- [11] I. Boztosun and W.D.M. Rae, *Phys. Lett.* **518B** (2001) 229.
- [12] A.M. Kobos and G.R. Satchler, *Nucl. Phys.* **A427** (1984) 589.
- [13] V.N. Bragin and R. Donangelo, *Nucl. Phys.* **A433** (1985) 495.
- [14] W. Sciani, A. Lepine-Szily, F.R. Lichtenthailer, P. Fachini, L.C. Gomes, G.F. Lima, M.M. Obuti, J.M. Jr Oliveira and A.C.C. Villari, *Nucl. Phys.* **A620** (1997) 91.
- [15] R.L. Filho, A. LépineSzily, A.C.C. Villari and O.P. Filho, *Phys. Rev. C* **39** (1989) 884.
- [16] R.G. Stokstad, R.M. Wieland, G.R. Satchler, C.B. Fulmer, D.C. Hensley, S. Raman, L.D. Rickertsen, A.H. Snell and P.H. Stelson, *Phys. Rev. C* **20** (1979) 655.
- [17] M.E. Brandan and G.R. Satchler, *Phys. Reports* **285** (1997) 143.
- [18] J. Carter, R.G. Clarkson, V. Hnizdo, R.J. Keddy, D.W. Mingay, F. Osterfeld and J.P.F. Sellschop, *Nucl. Phys.* **A273** (1976) 523.
- [19] J. Carter, J.P. Sellschop, R.G. Clarkson and V. Hnizdo, *Nucl. Phys.* **A297** (1978) 520.
- [20] S.Y. Lee, *Nucl. Phys.* **A311** (1978) 518.
- [21] D.M. Brink and N. Takigawa, *Nucl. Phys.* **A279** (1977) 159.
- [22] P.D. Kunz, CHUCK, a coupled-channels code, unpublished.
- [23] A. Dudek-Ellis, V. Shkolnik and D. Dehnhard, *Phys. Rev. C* **18** (1978) 1039.
- [24] G.R. Satchler, *Direct Nuclear Reactions* (Oxford University Press, Oxford 1983) and *Introduction to Nuclear Reactions* (The Macmillan Press Ltd, London 1980).
- [25] G.V. Marti, A.J. Pacheco, J.E. Testoni, D. Abriola, O.A. Capurro, D.E. Di-Gregorio, J.O. Fernandez-Niello, E. Achterberg and D.E. Alvarez, *Phys. Lett.* **447B** (1999) 41.
- [26] S.J. Sanders, M. Paul, J. Cseh, D.F. Geesaman, W. Henning, D.G. Kovar, R. Kozub, C. Olmer and J.P. Schiffer, *Phys. Rev. C* **21** (1810) 1980.
- [27] M.A. Franey, V. Shkolnik and D. Dehnhard, *Phys. Lett.* **81B** (1979) 132.
- [28] P.M. Endt and C. van der Leun, *Nucl. Phys.* **A214** (1973) 1.
- [29] D. Schwalm, E.K. Warburton and J.W. Olness, *Nucl. Phys.* **A293** (1977) 425.



TABLES

$E_{Lab}$	Standard CC	New CC
29.34	2.5	3.7
29.92	2.1	3.5
30.70	3.0	3.4
31.63	2.7	4.1
32.75	1.7	2.7
33.17	3.3	3.0
33.89	3.2	2.3
35.04	13.7	3.3
35.69	13.5	8.9
38.20	46.0	11.7
41.17	127.0	29.4

TABLE I. The numerical values of  $\chi^2$  for the standard and new CC cases in the inelastic scattering calculations.

$E_{Lab}$ (MeV)	$J_{W_S}$ (MeV fm <sup>3</sup> )	$J_{W_V}$ (MeV fm <sup>3</sup> )
29.34	3.23	0.25
29.92	3.59	0.27
30.70	4.12	0.31
31.63	4.81	0.35
32.75	5.75	0.40
33.17	6.13	0.42
33.89	6.82	0.45
35.04	8.03	0.52
35.69	8.78	0.56
38.20	12.10	0.73
41.17	17.02	0.97

TABLE II. The volume integrals of the surface and volume imaginary potentials for the new coupled-channels calculations. The volume integral of the real potential is 381.9 MeV fm<sup>3</sup>

## FIGURES

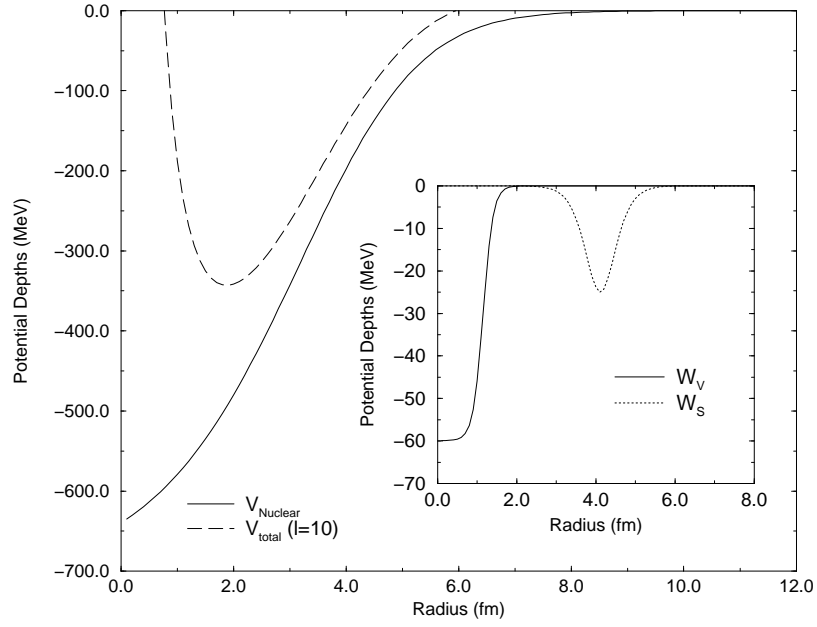


FIG. 1. The real and imaginary parts of the potential between  $^{16}\text{O}$  and  $^{28}\text{Si}$  are plotted against the separation  $R$  for  $l=10$ .  $W_V$  denotes the volume and  $W_S$  the surface components of the imaginary potential at  $E_{\text{Lab}}=41.17$  MeV (the inserted figure).

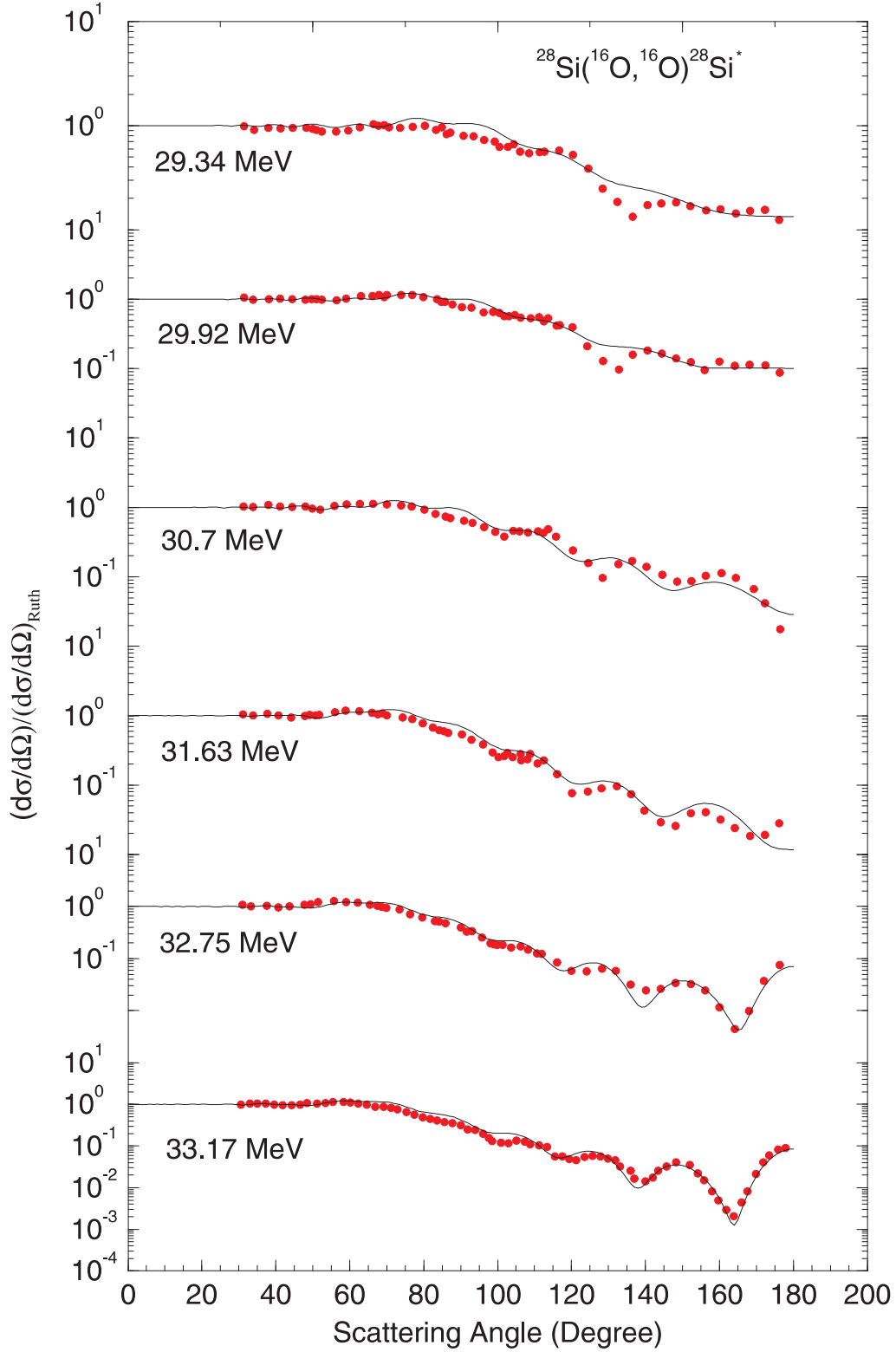


FIG. 2. Ground state results obtained using the standard coupled-channels model with  $\beta_2=-0.64$ .

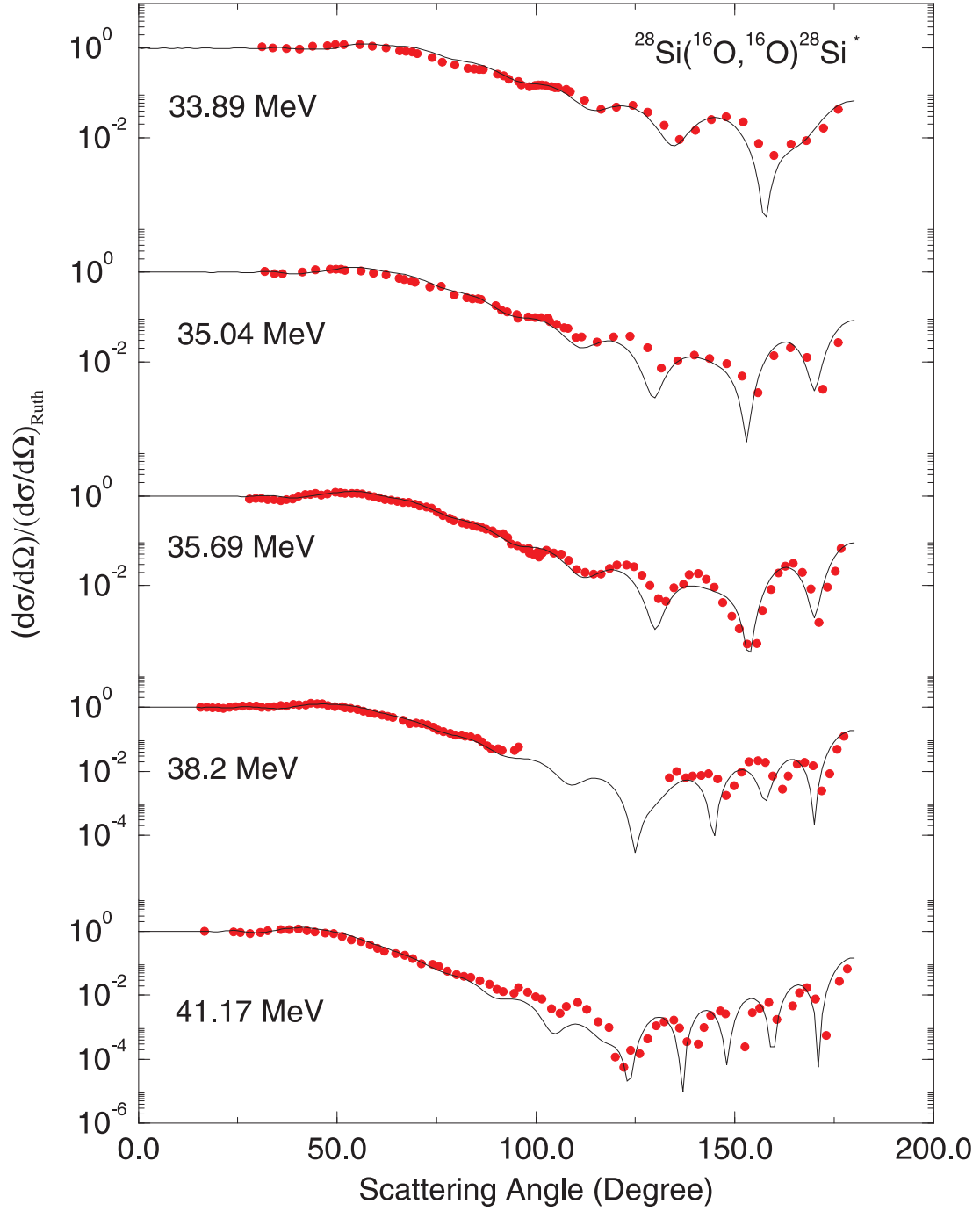


FIG. 3. Ground state results obtained using the standard coupled-channels model with  $\beta_2=-0.64$  (continued from figure 2).

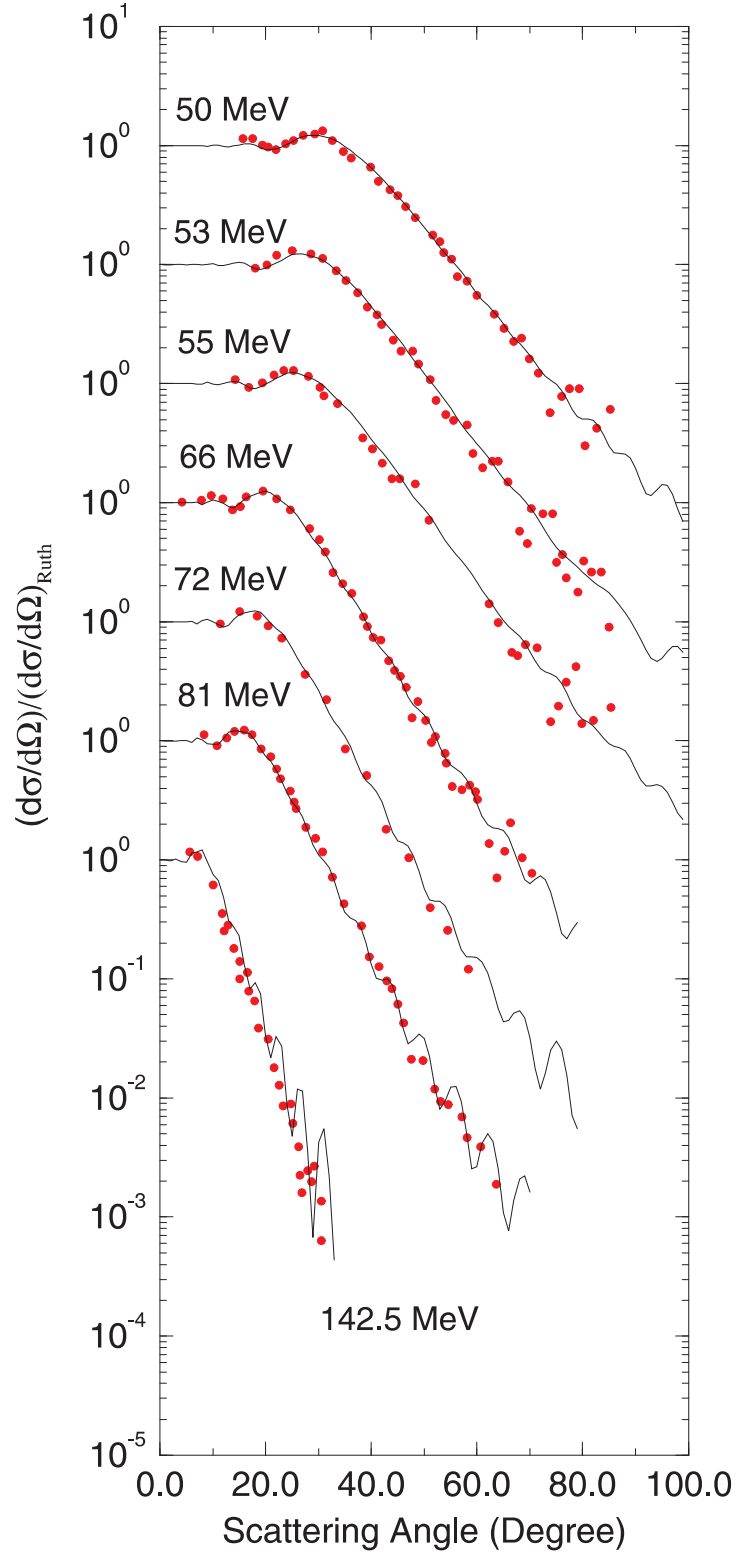


FIG. 4. Ground state results obtained using the standard coupled-channels model with  $\beta_2=-0.64$  (continued from figure 3).

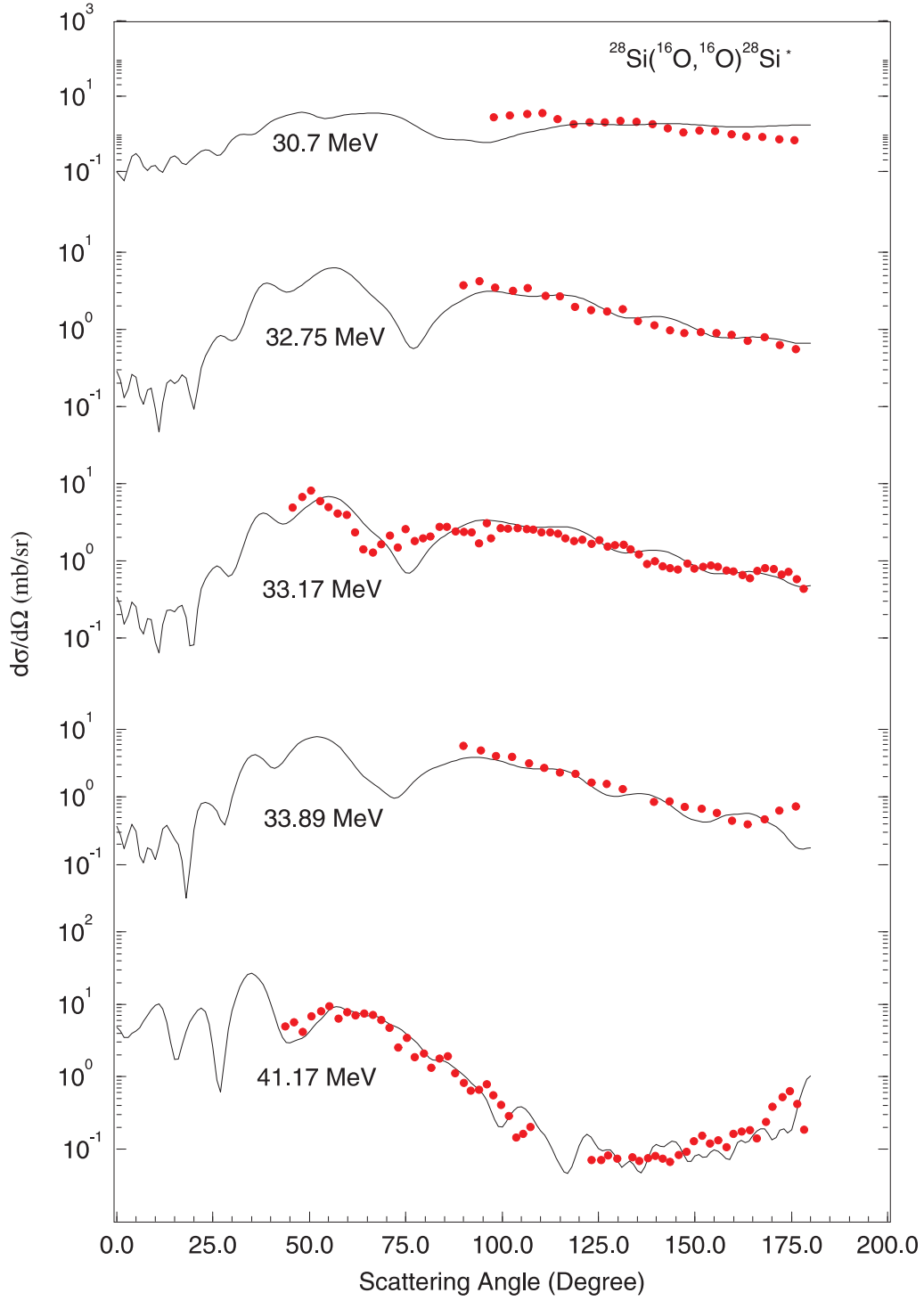


FIG. 5.  $2^+$  excited state results obtained using the standard coupled-channels model with  $\beta_2=-0.64$ .

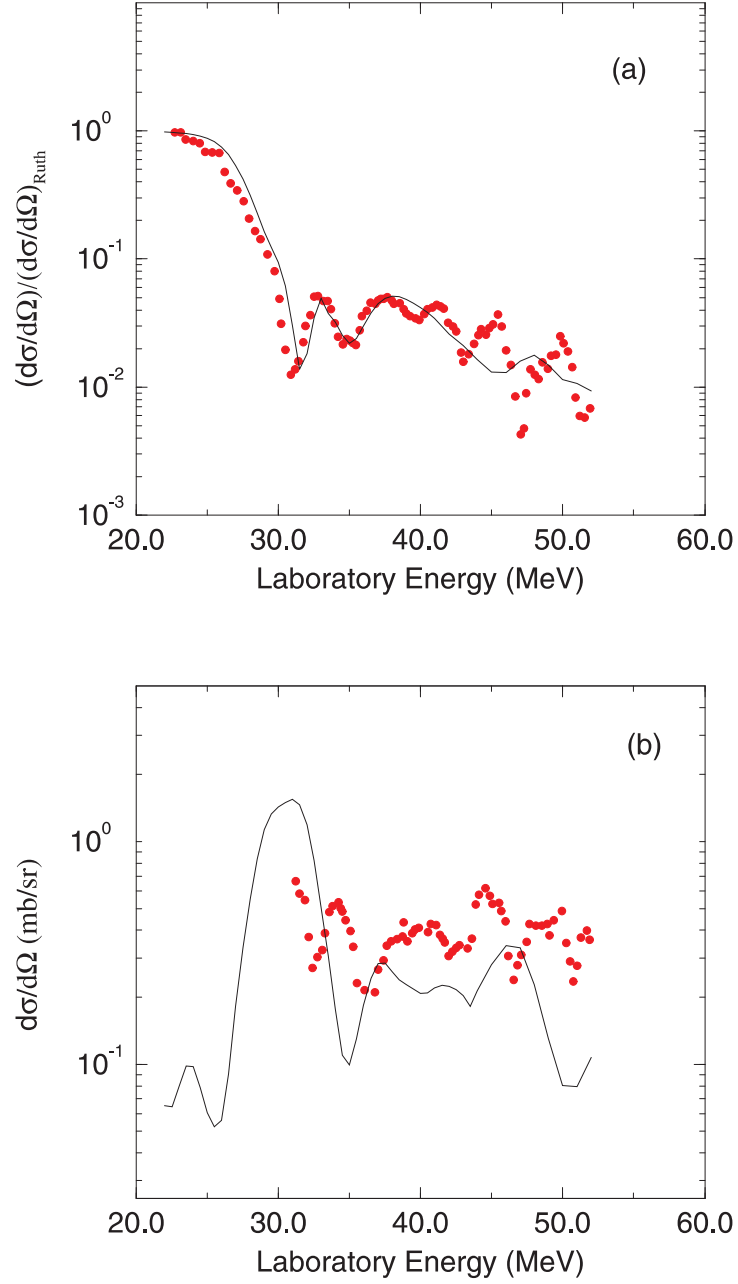


FIG. 6.  $180^\circ$  excitation function results obtained using the standard coupled-channels model for (a) the ground and (b)  $2^+$  states with  $\beta_2=-0.64$ .

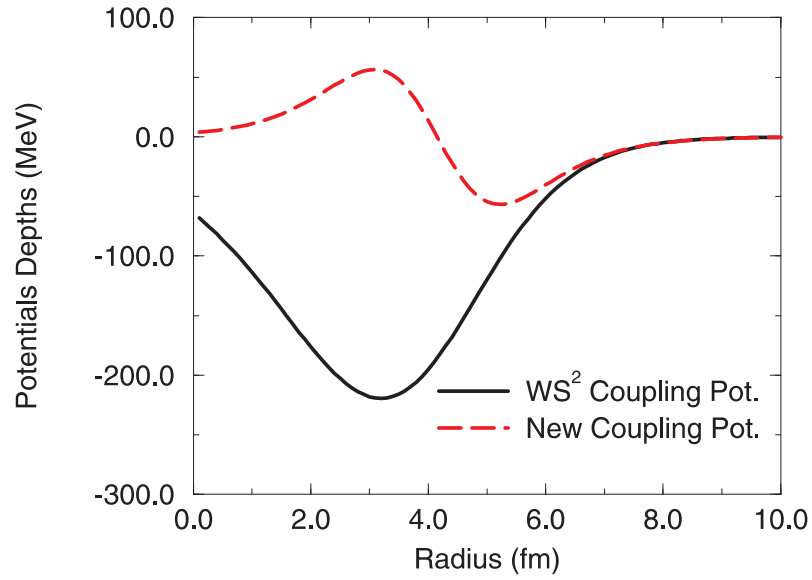


FIG. 7. The comparison of the *standard* coupling potential and our *new* coupling potential, parameterized as the 2<sup>nd</sup> derivative of Woods-Saxon shape.



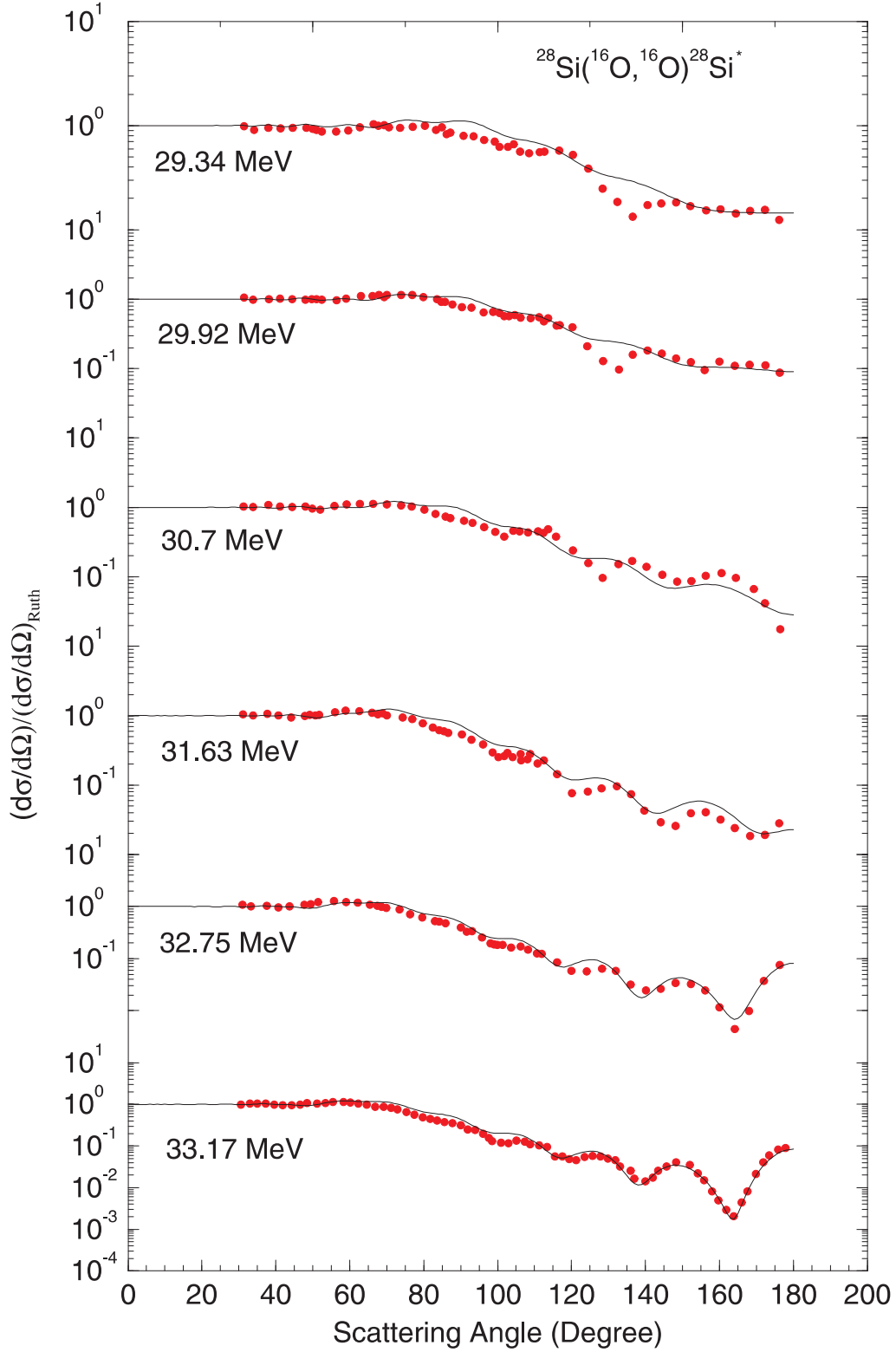


FIG. 8. Ground state results obtained using the new coupling potential with the exact  $\beta$  value.

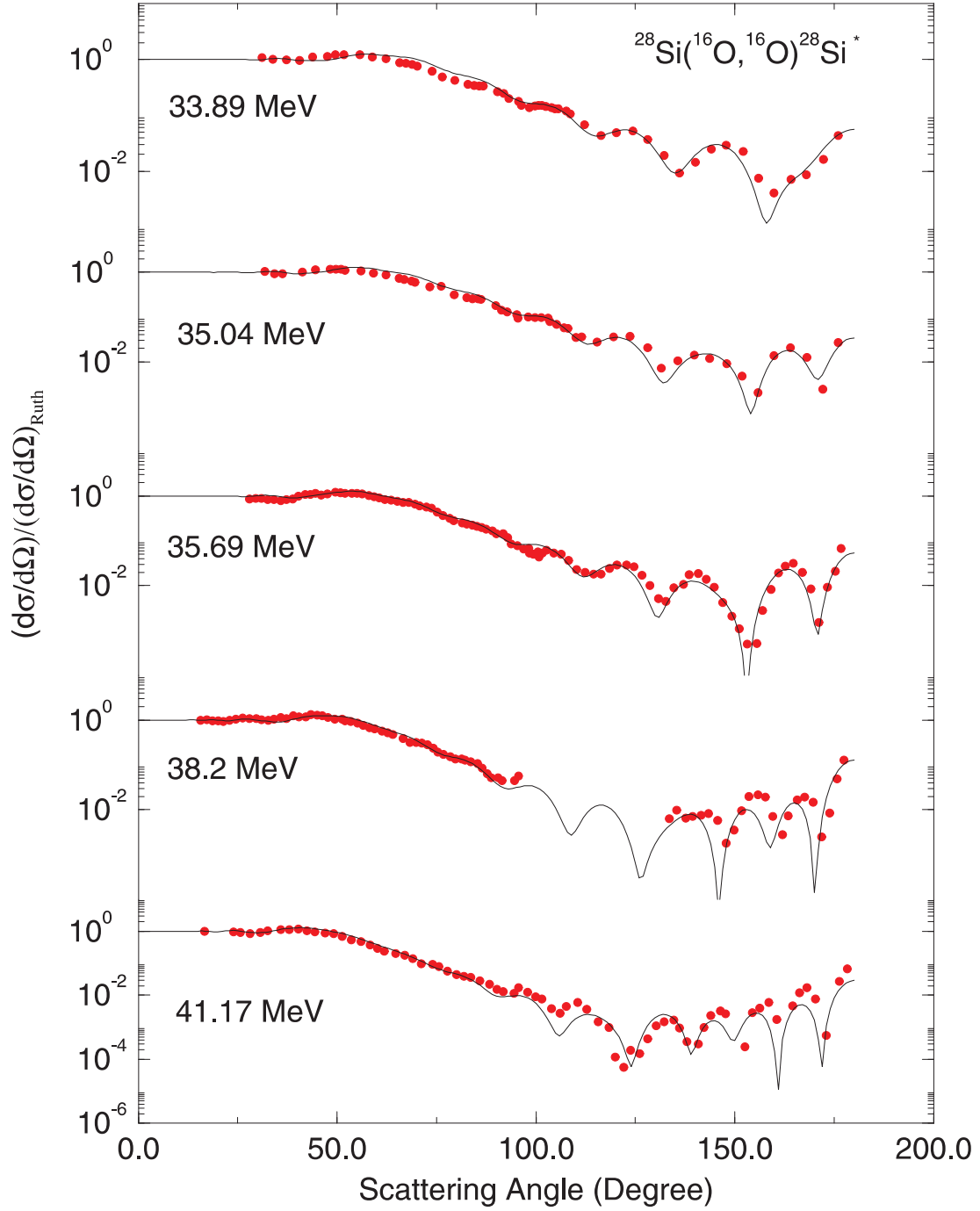


FIG. 9. Ground state results obtained using the new coupling potential with the exact  $\beta$  value (continued from figure 8).

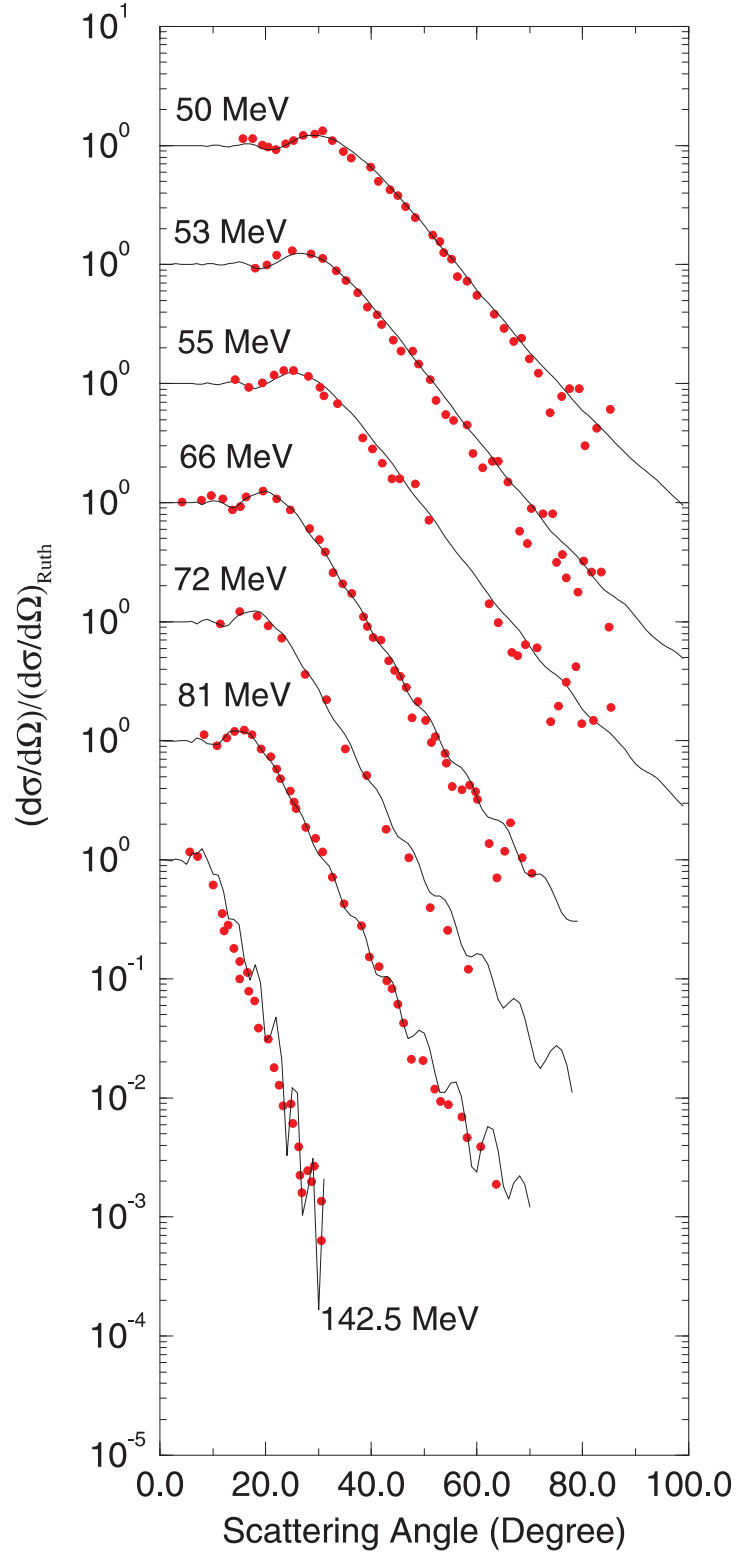


FIG. 10. Ground state results obtained using the new coupling potential with the exact  $\beta$  value (continued from figure 9).

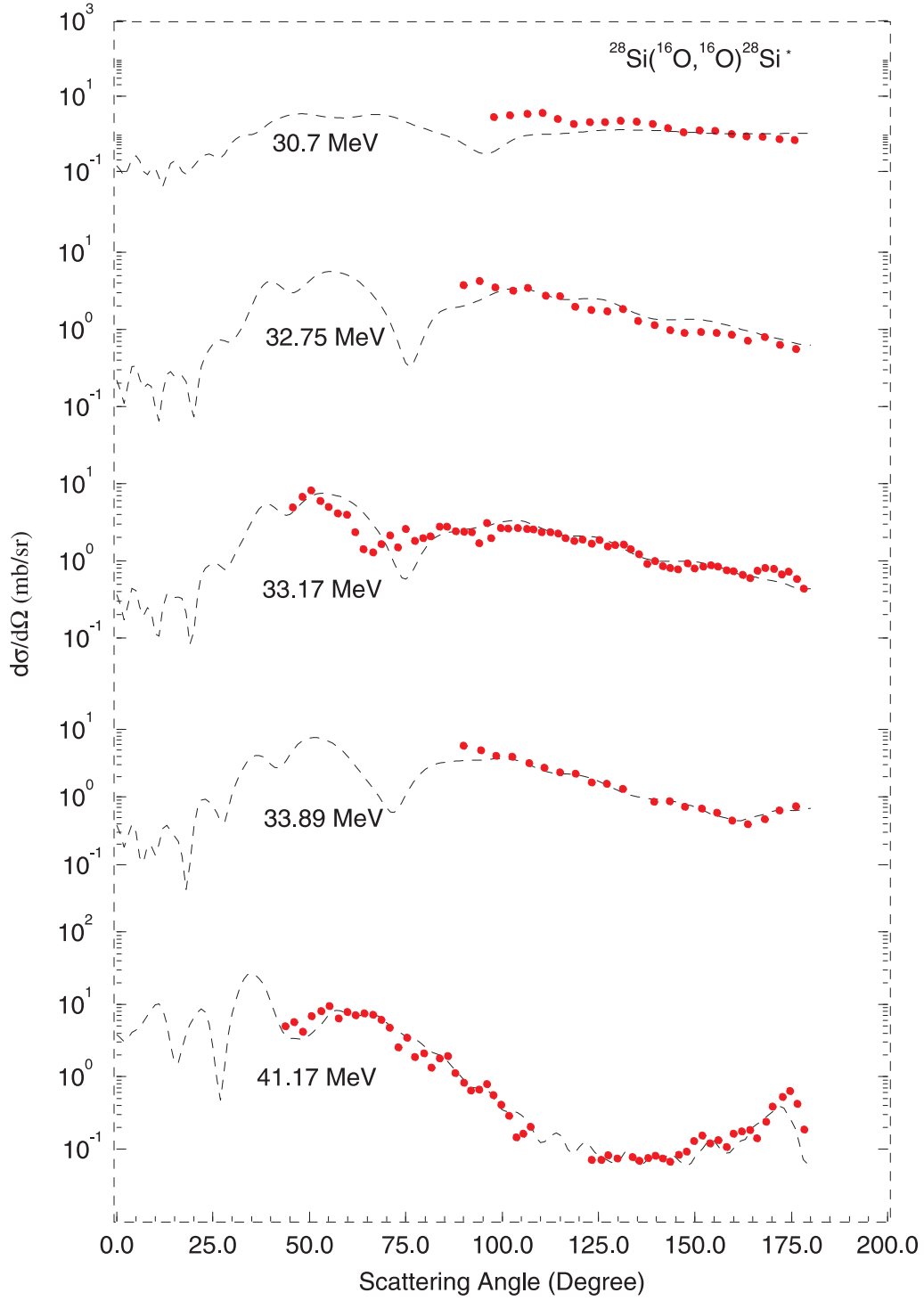


FIG. 11.  $2^+$  excited state results obtained using the new coupling potential with the exact  $\beta$  value.

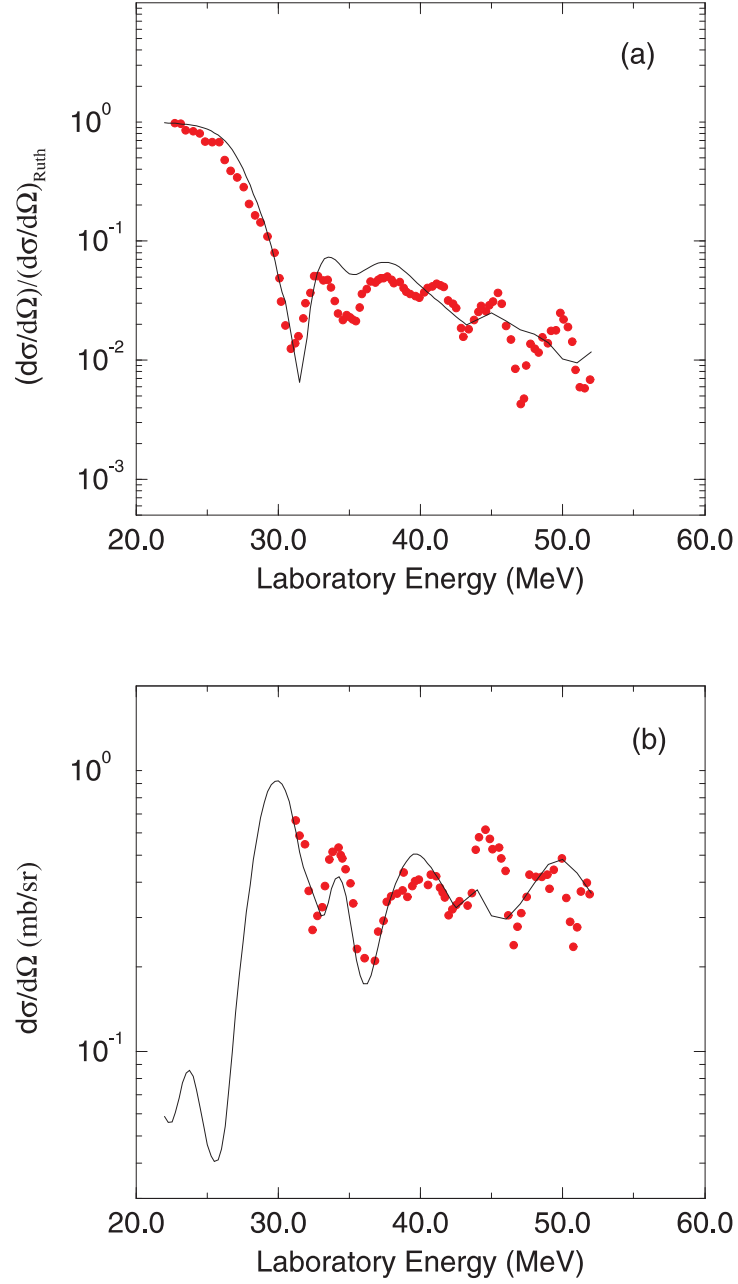


FIG. 12.  $180^\circ$  excitation function results obtained using the new coupling potential with the exact  $\beta$  value for (a) the ground and (b)  $2^+$  states.